Applied Acoustics 199 (2022) 109019

Contents lists available at ScienceDirect

Applied Acoustics

journal homepage: www.elsevier.com/locate/apacoust

Plate-type acoustic metamaterials with integrated Helmholtz resonators

F. Langfeldt [a,b,*], A.J. Khatokar [b], W. Gleine [b]

[a] Institute of Sound and Vibration Research, University of Southampton, University Road, Southampton SO17 1BJ, United Kingdom
[b] Department of Automotive and Aeronautical Engineering, Hamburg University of Applied Sciences, Berliner Tor 7a, D-20099 Hamburg, Germany

ARTICLE INFO

Article history:
Received 18 March 2022
Received in revised form 27 June 2022
Accepted 1 September 2022

Keywords:
Acoustic metamaterial
Helmholtz resonator
Transmission loss
Experiment
Simulation

ABSTRACT

Plate-type acoustic metamaterials (PAM) consist of a thin film with periodically added masses. These metamaterials can be designed to be very lightweight and exhibit narrow bands at low frequencies with high sound transmission loss values that can exceed the corresponding mass-law considerably. In this paper, a new approach for improving the bandwidth of PAM by using Helmholtz resonators which represent the added masses is investigated. The key principle of this design is that the Helmholtz resonance gives rise to an additional peak in the transmission loss spectrum which can be tuned to increase the bandwidth of the PAM. Sound transmission loss measurements of a large-scale test sample with 270 resonators are used to demonstrate the performance of the proposed metamaterial under diffuse field excitation. Then, numerical simulations based on the finite element method are used to further investigate the physical mechanisms of the PAM with Helmholtz resonators. It is shown that when the baseplates of the Helmholtz resonators are stiff enough, the Helmholtz resonance is decoupled from the vibroacoustics of the PAM. This can be exploited to effectively increase the bandwidth of PAM without any significant reductions of the sound transmission loss due to coupling resonances.

1. Introduction

Helmholtz resonators (HR) have been used in a broad range of applications within noise control, for example as low frequency sound absorbers in rooms [1] or to increase the sound transmission loss of double wall partitions [2]. Recently, it has also been demonstrated that acoustic metamaterials with Helmholtz resonators can exhibit frequency bands with negative bulk modulus, which can be exploited in noise control applications or the development of acoustic cloaks [3,4]. The sound transmission loss of a metamaterial plate with integral Helmholtz resonators was investigated in Ref. [5], where it could be shown that the sound transmission loss (STL) of the plate can be significantly increased at the resonance frequency of the Helmholtz resonators. Plate-type acoustic metamaterials (PAM), on the other hand, are composed of a thin baseplate with periodically attached masses. As first demonstrated by [6], PAM can exhibit narrow frequency bands (so-called anti-resonances) in the low frequency range with STL values significantly surpassing the corresponding mass-law values. This makes PAM a promising solution for noise control problems with strong weight limitations on noise reduction materials. Since the investigations by [6] and the advent of acoustic metamaterials in the 2000s, more thorough investigations of PAM have been published [7,8]. For example, [9] used an analytical model to calculate the sound transmission and bending wave energy propagation of PAM with point-like masses. In Ref. [10], the effect of inaccuracies in the parameters of the periodically added masses (e.g. random mass positions) was investigated numerically. It could be shown that such inaccuracies can lead to a damping-like smoothing of the STL spectrum of PAM. [11] provide a parametric study using a semi-analytical model to investigate the effect of different PAM design parameters on the STL properties of PAM. Their model was validated using sound intensity measurements under diffuse sound field excitation.

The typically narrow bandwidth of the anti-resonances of PAM somewhat limits their application to noise sources with fixed tonal components. Therefore, some effort has been made recently to increase the bandwidth of PAM and thus expand the range of potential applications of PAM in noise control. [12] studied experimentally the structure-borne sound transmission of a PAM with resonant tungsten/silicone rubber stubs. They could show that due to the resonances of the stubs a broad band-gap with significantly reduced vibration amplitudes forms at frequencies below 3 kHz. The STL properties of a PAM with multi-resonant stubs were studied using simulations by [13]. They could show that multiple anti-resonances could be introduced by this method, leading to

* Corresponding author at:Institute of Sound and Vibration Research, University of Southampton, University Road, Southampton SO17 1BJ, United Kingdom.
E-mail addresses: F.Langfeldt@soton.ac.uk (F. Langfeldt), Wolfgang.Gleine@haw-hamburg.de (W. Gleine).

https://doi.org/10.1016/j.apacoust.2022.109019
0003-682X/

an improved bandwidth. In Refs. [14,15] two layers of PAM were coupled with a tonraum resonator in order to enhance the bandwidth of the PAM. [16] demonstrated using a generalized analytical model that the bandwidth of PAM can be increased by using multiple masses in one unit cell or by stacking multiple PAM layers. Using optimizations, it was also shown that, for a fixed overall surface mass density of the PAM, there exists a certain maximum bandwidth that cannot be exceeded, unless additional masses and/or PAM layers are introduced.

This paper investigates a new approach to increasing the bandwidth of PAM anti-resonances. The present approach distinguishes itself from previous attempts by replacing the solid or composite masses with Helmholtz resonators, which exhibit acoustic resonances at their respective Helmholtz resonance frequencies f_R. Fig. 1(a) shows the basic setup of the PAM with Helmholtz resonator masses arranged in a square array with a unit cell size of a. A cross-section of one unit cell with the geometrical parameters of the Helmholtz resonators and the baseplate is shown in Fig. 1(b). The key motivation for this new PAM design with Helmholtz resonator masses is that the anti-resonance of the PAM and the Helmholtz resonance can be combined to improve the bandwidth of PAM.

2. Sound transmission loss measurement

2.1. Methodology

A 1 m × 1.2 m large test sample was built in order to perform STL measurements of a PAM with Helmholtz resonator masses under diffuse sound field excitation in a reverberation chamber/hemi-anechoic chamber test setup, as illustrated in Fig. 2(a). The sample was composed of a $t = 0.55$ mm thick polycarbonate (PC) plate with $15 \times 18 = 270$ Helmholtz resonator masses glued onto it in a square array with a unit cell size of $a = 65$ mm using a

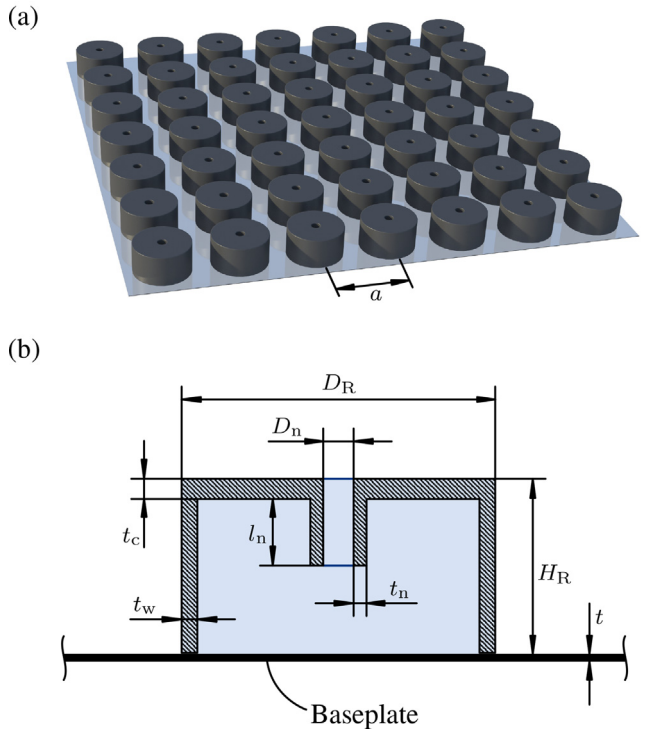

Fig. 1. (a) Plate-type acoustic metamaterial (PAM) with Helmholtz resonator masses arranged in a square periodic array (unit cell size: a); (b) Cross-section and geometrical parameters of one unit cell.

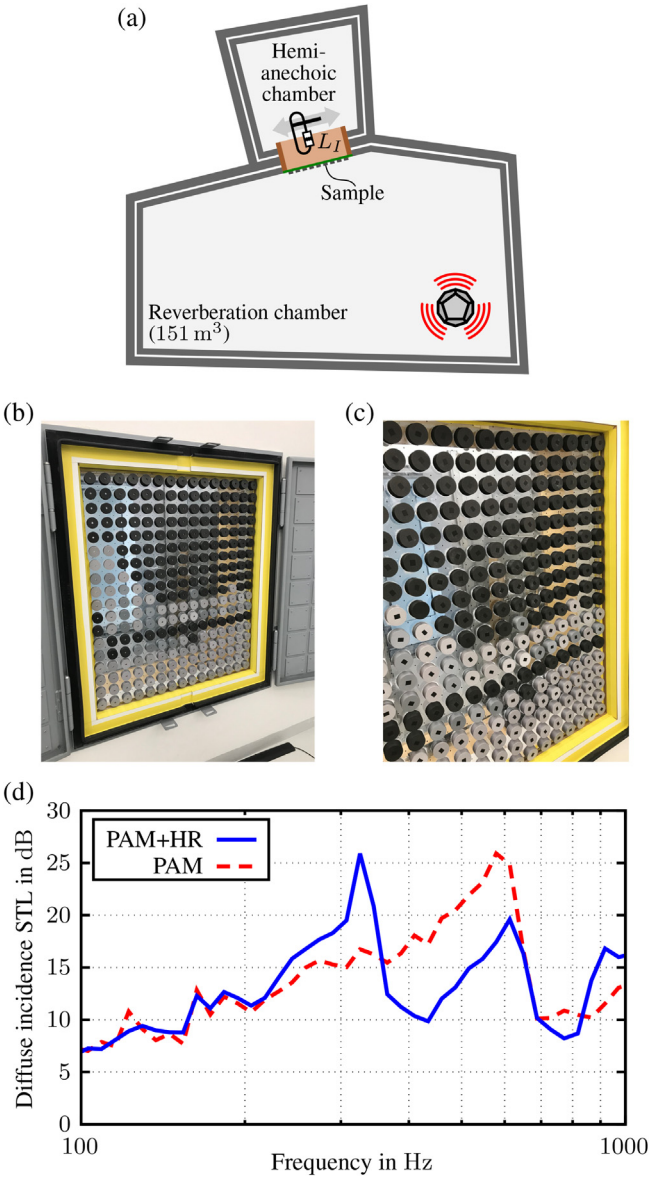

Fig. 2. (a) Overview of the sound intensity measurement setup; (b) 1 m × 1.2 m large experimental test sample of a plate-type acoustic metamaterial with 270 Helmholtz resonator masses (PAM + HR); (c) Test sample with the Helmholtz resonator necks closed using tape (PAM); (d) Measured diffuse incidence sound transmission loss of both configurations.

cyanoacrylate-based instant adhesive. Each Helmholtz resonator was additively manufactured using polylactic acid (PLA) and weighed 10 g. The outer diameter and height of each resonator were given by $D_R = 50$ mm and $H_R = 27$ mm, respectively. The diameter of the neck was $D_n = 8$ mm and the neck extended inside the cavity of each resonator by a length of $l_n = 8.5$ mm. The thicknesses of the resonator walls were $t_c = 1$ mm, $t_w = 1.5$ mm, and $t_n = 0.7$ mm for the cover, sides, and neck extension, respectively. Fig. 2(b) shows the test sample with open Helmholtz resonator necks mounted inside the transmission test window. Note that the different colours of the resonators were a result of differently dyed PLA used in the manufacturing process. All resonators have the same geometrical properties. In Fig. 2(c) it is shown how the Helmholtz resonator necks were closed using small pieces of adhesive tape in order to represent a conventional PAM with non-resonant masses. The added mass of the adhesive tape was, on average, 21mg per resonator, which corresponds to an increase

of the resonator mass by only 0.2%. Therefore, it was assumed that the impact of the mass of the adhesive tape on the performance of the PAM is negligible.

2.2. Results

The STL measurements were carried out using a sound intensity probe in accordance with a modified measurement method based on ISO 15186-2 [17]. For each sample, the measurement consisted of two steps: First, with no test sample present in the test window, the average incident sound intensity level $L_{I,\mathrm{in}}$ was measured by sweeping the intensity probe across the open window area. Then, the sample was mounted inside the window and the average transmitted sound intensity level $L_{I,\mathrm{tr}}$ was measured. In all of these measurements the white noise signal fed into the loudspeaker in the reverberation chamber remained unchanged. The transmission loss is then given by $\mathrm{TL} = L_{I,\mathrm{in}} - L_{I,\mathrm{tr}}$. This modified measurement method has been chosen because it provides more accurate results, especially at lower frequencies where the sound field in the reverberation chamber can be affected by room modes [17].

The measurement results are shown in Fig. 2(d) for the configurations with open Helmholtz resonators (PAM + HR) and closed resonators (PAM). For the PAM with closed Helmholtz resonators, the first anti-resonance can be clearly seen at 600 Hz with STL values of over 25 dB. When the Helmholtz resonators are open (PAM + HR), this anti-resonance remains at roughly the same frequency, but the peak STL value is reduced by approximately 5 dB. It will be shown later using the numerical simulations that this reduction is a consequence of the flexibility of the Helmholtz resonator baseplate and can be avoided by strengthening the baseplate. Additionally, a second STL peak can be observed at approximately 320 Hz, which corresponds to the acoustic resonance of the Helmholtz resonators. It should be noted that this frequency is considerably smaller than what would be expected when using well-known formulas for the resonance frequency of Helmholtz resonators (here: $f_{\mathrm{R}} \approx 460$ Hz). The reason for the reduced Helmholtz resonance frequency is the elasticity of the thin baseplate, which reduces the effective stiffness of the air volume inside the resonators [18]. In any case, these experimental results demonstrate that Helmholtz resonators can indeed be used as masses for PAM to introduce new anti-resonances. The additional anti-resonances result from making the PAM masses behave like a Helmholtz resonator, which does not increase the overall mass of the PAM or requires the use of mechanically resonating structures.

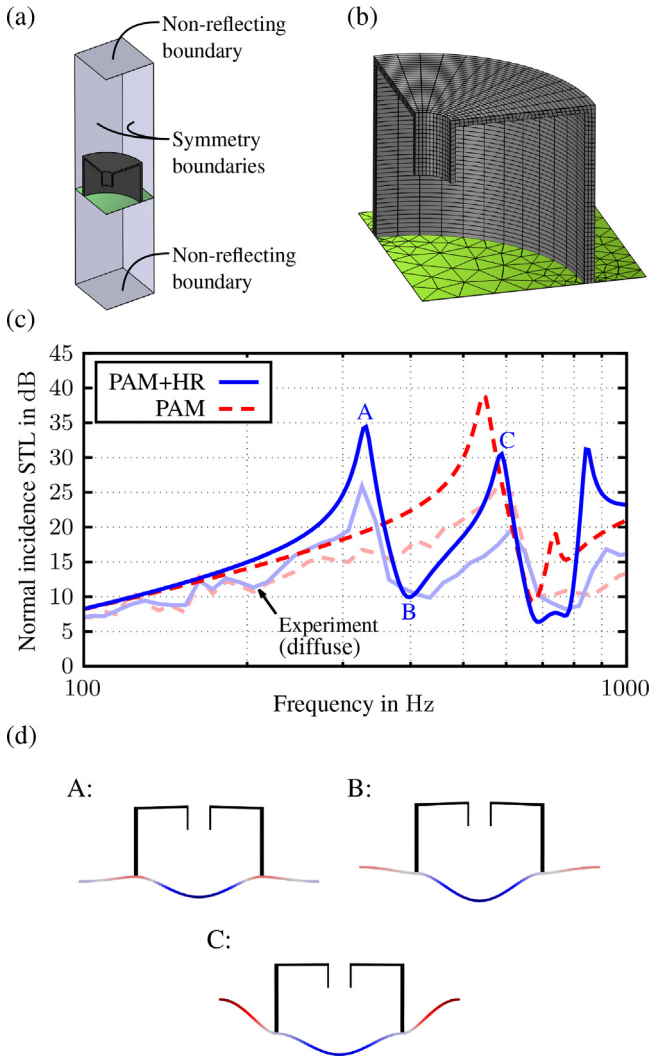

Fig. 3. (a) Schematic illustration of the simulation model of the PAM with Helmholtz resonator mass; (b) Detailed view of the baseplate and Helmholtz resonator meshing; (c) Simulated normal incidence STL of the PAM with HR and PAM with closed resonators configurations (the experimental results obtained under diffuse incidence are included for qualitative comparison); (d) Simulated displacement of the PAM with Helmholtz resonator mass at the characteristic frequencies labelled in (c).

3. Numerical investigation

3.1. Methodology

While the experimental results in the previous section clearly demonstrated that the introduction of the Helmholtz resonators leads to an additional peak in the STL spectrum, a few questions could not be answered using the experimental data—in particular, why the new STL peak did not appear at the predicted resonance frequency of the Helmholtz resonators. To further investigate the physical mechanisms behind the STL of the PAM with Helmholtz resonators, numerical simulations of a single unit cell have been performed using the finite element method (FEM). Normally incident plane acoustic waves were considered in the simulations and due to symmetry only one quarter of the unit cell was modelled with symmetry boundary conditions specified at the lateral surfaces (see Fig. 3(a)). Fluid domains were added to both sides of the PAM. These domains were truncated after about one unit cell length distance from the PAM using non-reflecting boundaries. Full vibro-acoustic coupling between the PAM and the surrounding fluid was considered in the simulations. The visco-thermal losses in the neck of the Helmholtz resonator were taken into account by modelling the fluid inside the neck as an equivalent fluid [19]. The PAM with closed Helmholtz resonators was modelled by closing the neck using an interior sound-hard boundary. For the numerical discretization, second order 3D elements were used for both the fluid and the Helmholtz resonator, while second order shell elements were used for the baseplate. Fig. 3(b) shows a detailed view of the mesh for the structural part of the model. In the meshing of the fluid domains it was ensured that the maximum element size is $a/6 \approx 10.8$ mm. The material properties used in the FEM simulations are specified in Table 1. The acoustic excitation was imposed using a plane acoustic wave travelling in the orthogonal direction to the baseplate. The resulting STL was obtained by integrating the transmitted intensity over a surface on the transmission side of the PAM to obtain the transmitted sound power W_{tr}. The STL is then given by $\mathrm{TL} = 10\log(W_{\mathrm{in}}/W_{\mathrm{tr}})$, where the incident sound power W_{in} can be calculated from the pressure amplitude of the incident sound wave.

Table 1
Material properties used in the FEM simulations.

	PC	PLA	Air	
Density	1210	1250	1.2	kg m^{-3}
Young's modulus	2200	3500	–	MPa
Shear modulus	800	1300	–	MPa
Loss factor	5	5	–	%
Speed of sound	–	–	343	m s^{-1}
Dynamic viscosity	–	–	18.1	μPa s
Ratio of specific heats	–	–	1.4	–
Prandtl number	–	–	.71	–

3.2. Results

The simulated normal incidence STL is shown in Fig. 3(c) for both configurations of the PAM with open and closed Helmholtz resonators. For a better qualitative comparison with the measurement data shown in Fig. 2(d), the experimental data has been included in Fig. 3(c) (light blue and light red curves). By comparing the numerical results with the measurement data qualitatively it can be seen that the simulation reproduces the main characteristics of the experimental results quite well. Note that the STL amplitudes in the simulations are generally higher than in the experiment, because normal incidence is considered here, while the experimental STL has been obtained under diffuse incidence. The frequencies of the peaks and dips in the STL curves, however, are very close to the values observed in the experiments. Minor deviations can be attributed to inaccuracies in the specifications of the material properties and manufacturing tolerances. The simulated displacement of the PAM is shown in Fig. 3(d) for the characteristic points in the STL curved labelled in Fig. 3(c). At point A, corresponding to the first anti-resonance, the resonator and most parts of the baseplate are vibrating out of phase, so that the surface-averaged displacement across the unit cell is near zero and, consequently, almost no sound is transmitted. At point B, however, the PAM exhibits a resonance with strong vibrations of the bottom of the Helmholtz resonator, while the other parts of the PAM are relatively at rest. Due to this resonance, the STL of the PAM is clearly reduced at this frequency. Point C corresponds to the second anti-resonance of the PAM with Helmholtz resonators, which is very close to the anti-resonance of the PAM with closed resonators. At this frequency, the resonator is at rest, while the resonator bottom and the baseplate material outside the resonator vibrate out of phase. Similar to point A, this results in a surface-averaged displacement of nearly zero and highly reduced sound transmission.

In all three cases it can be clearly seen that, owing to the small thickness of the baseplate, the bottom of the Helmholtz resonator exhibits strong vibrations. This leads to the reduced STL at point B, which is not observed in case of the PAM with closed resonators. To confirm that this effect is not simply caused by the ring shaped footprint of the Helmholtz resonator imposed onto the baseplate, an additional simulation has been performed with the Helmholtz resonator being replaced by a rigid ring with equal inner and outer diameters and mass. The results are not shown in Fig. 3(c) to keep the plots clear, but it can be summarized that the PAM with ring mass—similar to the PAM with closed HR—exhibits only a single anti-resonance (at a somewhat different anti-resonance frequency), which does not explain the two peaks and the dip in between, as observed in Fig. 3(c).

Since the resonance between the two anti-resonances at A and C impairs the sound insulation performance of the PAM with HR considerably, the effect of increasing the stiffness of the resonator base is studied numerically. For this purpose, additional simulations have been performed with the baseplate material inside the Helmholtz resonator being replaced by a perfectly rigid material with equal density. The results of this simulation are shown in Fig. 4(a). Here, it can be clearly seen that the STL of the PAM is not reduced by an additional resonance when the resonator base is rigid. In fact, when the Helmholtz resonator is active, the STL of the original PAM (with closed resonators) is almost unaltered, except for a region of pure STL improvement around the resonance frequency of the Helmholtz resonator $f_R \approx 460$ Hz. This demonstrates that when vibrations of the resonator base are prevented, the PAM and the Helmholtz resonator are uncoupled and their STL peaks are simply overlayed without any resonances appearing in between, according to the completely independent physical laws for the PAM and Helmholtz resonator mechanisms. This is a significant difference to other attempts for improving the bandwidth of PAM (e.g. by using multiple masses per unit cell or stacking multiple PAM layers), where the introduction of additional anti-resonances inevitably leads to resonances in between these anti-resonances [16]. Furthermore, this uncoupled behaviour could also be exploited to increase the STL of the PAM at its resonance frequency by tuning the Helmholtz resonators to this frequency.

To demonstrate the potential of increasing the bandwidth of PAM by using Helmholtz resonator masses, further simulations have been performed with varying neck lengths $l_n = 5.5$ mm to 11.5 mm. Note that in these simulations the resonator bases were kept rigid. The numerical results are shown in Fig. 4(b). Changing l_n mainly affects the Helmholtz resonance frequency—the anti-resonance of the PAM remains at around 550 Hz, because the neck extension of the Helmholtz resonator has a negligible influence on the overall weight of the resonator. When the neck length is increased, the Helmholtz resonance frequency is reduced and consequently the first STL peak in Fig. 4(b) (which is attributed to the Helmholtz resonance) moves to lower frequencies. If the Helm-

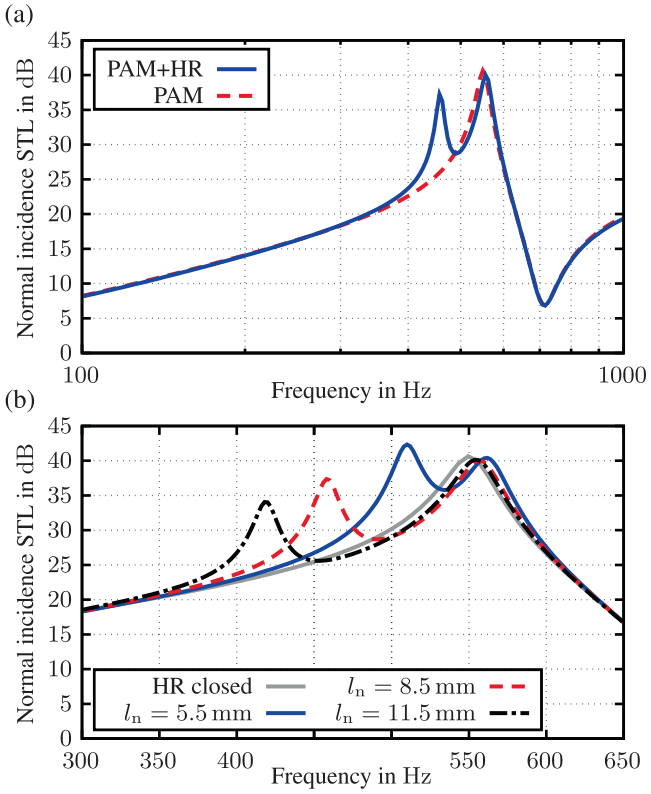

Fig. 4. (a) Simulated normal incidence STL of the PAM with HR and PAM with closed resonators configurations with rigid resonator bases; (b) Parametric study of changing the Helmholtz resonance frequency by using different neck lengths l_n (rigid resonator bases).

holtz resonance frequency and the PAM anti-resonance frequency are reasonably far apart, both STL peaks are clearly separated, which can be useful for multi-tonal noise sources. On the other hand, if the two frequencies are very close to each other (as in the case for $l_n = 5.5$ mm), the two peaks essentially merge into a single broader peak, effectively increasing the bandwidth of the PAM.

4. Conclusions

In summary, the sound reduction of a plate-type acoustic metamaterial with Helmholtz resonator masses was studied in this paper. Sound transmission loss measurements of a large-scale test sample demonstrated the acoustic performance of the proposed metamaterial under diffuse sound field excitation. It could be observed that additional peaks can be introduced in the STL spectrum, which can be attributed to the Helmholtz resonance of the masses. Numerical simulations have been used to demonstrate that the Helmholtz resonance and the PAM anti-resonance can be effectively decoupled when the baseplate of the Helmholtz resonators is sufficiently rigid. It is then possible to significantly broaden the bandwidth of the PAM by tuning the Helmholtz resonance frequency close to the PAM anti-resonance frequency. This broadened bandwidth comes along without any additional mass and significant reduction of the STL, as compared to a mass-equivalent PAM without Helmholtz resonators.

CRediT authorship contribution statement

F. Langfeldt: Conceptualization, Methodology, Validation, Formal analysis, Visualization, Writing - original draft, Writing - review & editing, Supervision. **A.J. Khatokar:** Validation, Investigation, Writing - review & editing. **W. Gleine:** Resources, Writing - review & editing, Supervision, Funding acquisition.

Declaration of Competing Interest

The authors declare that they have no known competing financial interests or personal relationships that could have appeared to influence the work reported in this paper.

Acknowledgements

This work was supported by the Federal Ministry for Economic Affairs and Climate Action [Grant No. 20Q1908D].

References

[1] Fahy FJ, Schofield C. A note on the interaction between a Helmholtz resonator and an acoustic mode of an enclosure. J Sound Vib 1980;72:365–78.
[2] Mason JM, Fahy FJ. The use of acoustically tuned resonators to improve the sound transmission loss of double-panel partitions. J Sound Vib 1988;124:367–79.
[3] Fang N, Xi D, Xu J, Ambati M, Srituravanich W, Sun C, Zhang X. Ultrasonic metamaterials with negative modulus. Nat Mater 2006;5:452–6.
[4] Cummer SA, Christensen J, Alù A. Controlling sound with acoustic metamaterials. Nature Rev Mater 2016;1:16001.
[5] Yamamoto T. Acoustic metamaterial plate embedded with Helmholtz resonators for extraordinary sound transmission loss. J Appl Phys 2018;123:215110.
[6] Kurtze G. Light-weight walls with high transmission loss. Acta Acustica united with Acustica 1959;9:441–5.
[7] Huang T-Y, Shen C, Jing Y. Membrane- and plate-type acoustic metamaterials. J Acoust Soc Am 2016;139:3240–50.
[8] Ma F, Wang C, Liu C, Wu JH. Structural designs, principles, and applications of thin-walled membrane and plate-type acoustic/elastic metamaterials. J Appl Phys 2021;129:231103.
[9] W. Maysenhölder, Bending-Wave Energy Propagation in Inhomogeneous Thin Plates and Membranes, in: Proceedings of Inter-Noise 2004, Prague, 2004, pp. 3465–4151.
[10] Langfeldt F, Gleine W. Impact of Manufacturing Inaccuracies on the Acoustic Performance of Sound Insulation Packages with Plate-Like Acoustic Metamaterials. SAE Int J Adv Curr Pract Mob 2020;3:1092–100.
[11] Xiao Y, Cao J, Wang S, Guo J, Wen J, Zhang H. Sound transmission loss of plate-type metastructures: Semi-analytical modeling, elaborate analysis, and experimental validation. Mech Syst Signal Process 2021;153:107487.
[12] Assouar MB, Senesi M, Oudich M, Ruzzene M, Hou Z. Broadband plate-type acoustic metamaterial for low-frequency sound attenuation. Appl Phys Lett 2012;101:173505.
[13] Zhou X, Wang L, Qin L, Peng F. Improving sound insulation in low frequencies by multiple band-gaps in plate-type acoustic metamaterials. J Phys Chem Solids 2020;146:109606.
[14] Ang LYL, Koh YK, Lee HP. Plate-type acoustic metamaterial with cavities coupled via an orifice for enhanced sound transmission loss. Appl Phys Lett 2018;112:051903.
[15] Ang LYL, Koh YK, Lee HP. Plate-type acoustic metamaterials: Evaluation of a large-scale design adopting modularity for customizable acoustical performance. Appl Acoust 2019;149:156–70.
[16] Langfeldt F, Gleine W. Optimizing the bandwidth of plate-type acoustic metamaterials. J Acoust Soc Am 2020;148:1304–14.
[17] O. Robin, A. Berry, Alternative methods for the measurement of panel transmission loss under diffuse acoustic field excitation, in: Proceedings of Inter-Noise 2016, Hamburg, 2016, pp. 3349–3358.
[18] Nudehi SS, Duncan GS, Farooq U. Modeling and Experimental Investigation of a Helmholtz Resonator With a Flexible Plate. J Vib Acoust 2013;135:041102.
[19] Blackstock DT. Fundamentals of Physical Acoustics. New York: John Wiley & Sons Ltd; 2000.